

RESEARCH ARTICLE

Experimental study of perturbation growth in a round laminar jet

Linar Gareev  | Vasily Vedeneev | Oleg Ivanov | Julia Zayko | Denis Ashurov | Alexander Reshmin | Vladimir Trifonov

Institute of Mechanics, Lomonosov
Moscow State University, Moscow, Russia

Correspondence

Linar Gareev, Institute of Mechanics,
Lomonosov Moscow State University, 1
Michurinskiy Avenue, Moscow, 119192,
Russia.
Email: gareev.lr@yandex.ru

Funding information

Russian Science Foundation,
Grant/Award Number: 20-19-00404

Abstract

Jet flows have many applications in various technical processes such as temperature control, mixing, spraying and so forth. Along with wide usage in technology and manufacturing, jet flows are the object of fundamental scientific interest. In particular, a proper understanding of laminar-turbulent transition in jets is highly important. In this experimental work, we study round laminar submerged jet flow of air and the evolution of controlled perturbations. First, the modal perturbation growth mechanism was under consideration. Thin metal rings were put into the jet at a small distance from the orifice to amplify unstable eigen modes of the jet by oscillating at different frequencies. Experimental and theoretically predicted wavelengths, radial distributions of velocity fluctuations and amplification curves of modal perturbations were compared and a good correspondence was found. Second, the non-modal perturbation growth mechanism was under consideration. To excite algebraic perturbation growth, we put special wavy structures (deflectors) into the jet, which provide a roller-like transverse motion in the perturbed jet. The features of the transition to turbulence caused by this non-modal growth were considered. Based on obtained experimental results, we definitely identify the non-modal ‘lift-up’ growth mechanism of introduced disturbances. The development of perturbations qualitatively corresponds to the theoretically calculated optimal perturbations.

1 | INTRODUCTION

Submerged jets are widely used in technological processes. The stability of jets and the transition to turbulence play an important role in many applications. It is believed that submerged laminar jets are unstable in practice because of their low critical Reynolds number, which does not exceed 40 [1–3]. In fact, such jets have a relatively small region (of the order of 1–2 orifice diameters in length) in which they retain a laminar structure. For this reason, it is extremely difficult to experimentally study the mechanisms of perturbations’ growth in the laminar region using conventional jets. The understanding of such mechanisms would definitely shed light on the roots of the laminar-turbulent transition and provide well-grounded control strategies for the transition.

In laminar jets, there is no doubt that the modal growth of perturbations plays a primary role in their transition to turbulence. It yields the formation of Kelvin–Helmholtz billows, visible in all experimental and numerical studies, and their further breakdown. However, the only experiments by Refs. [4, 5] on controlled excitation of a laminar portion of the

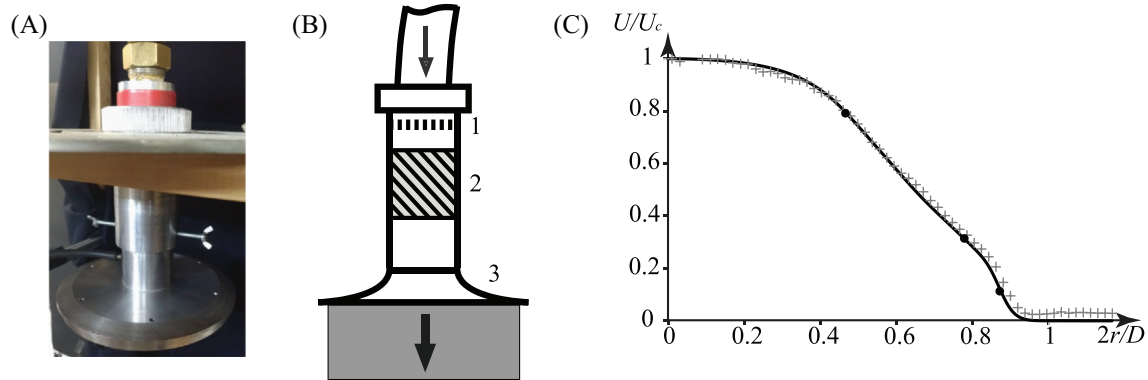


FIGURE 1 The photo of the jet forming device (A), scheme of this device (B): perforated plate (1), bushing with two different types of grids (2), diffuser with grid package at the orifice (3) and the velocity profile of a forming jet (C). The crosses show the experimental values obtained by the hot-wire anemometer; the solid line shows the profile used in theoretical analysis.

jet suffer from a very short laminar region (shorter than one diameter), which did not allow measuring wavelengths and spatial growth rates within the laminar region. Given that, on the one hand, experiments on perturbation growth should be conducted with sufficiently thick jets to be able to perform detailed experimental measurements of perturbations and that, on the other hand, the distance to transition should be sufficiently long to capture at least several wavelengths, it is extremely difficult to organize such laminar jet flow.

The situation has changed, as the setup described by Zayko et al. [6], creates submerged air jets with an essentially longer laminar region, $5D$ and more in length, where D is the orifice diameter. This unique facility allowed us to introduce two different types of controlled perturbations and to track their downstream evolution and its parameters. Using the modal stability theory [7], we obtained the numerical values of wavelengths of growing perturbations, the amplification curves and the radial distributions of perturbations. The same parameters were successfully measured experimentally.

The second part of this investigation has been devoted to the non-modal perturbation growth in the considered jet flow. It is well known that in addition to the modal linear growth mechanism in near-wall flows, there are two non-modal linear growth mechanisms [8]: the Orr mechanism and the “lift-up” mechanism. While the first is a purely two-dimensional process and leads to a relatively weak growth, the second, “lift-up”, gives a much stronger growth of three-dimensional disturbances and is responsible for the bypass transition in near-wall flows [9–11]. Streaky structures were experimentally studied in near-wall boundary layers, where they are associated with the bypass mechanism of transition to turbulence [12–16]. In unbounded flows, including submerged jets, the theoretical analysis of non-modal growth mechanism started only in the last decade [17–19]. In experiments, this mechanism has not been identified yet.

In order to excite non-modal (algebraic) perturbation growth, having the jet with long laminar region, we put special wavy structures (deflectors) into the jet, which provide a roller-like transverse motion. The features of the transition to turbulence caused by this non-modal growth were considered. Based on obtained experimental results, we definitely identify the non-modal ‘lift-up’ growth mechanism of introduced disturbances. The development of perturbations was tracked and compared with the theoretically calculated optimal perturbations [20].

2 | THE LAMINAR JET AND EXPERIMENTAL METHODS OF CONTROLLED PERTURBATIONS INTRODUCTION TO IT

2.1 | Jet forming device

In this study, we consider a laminar jet flow, which is formed by a device that consists of three parts (Figure 1A,B). The first part is a perforated plate that smooths out the stream incoming from the air pipeline (the diameter of the inlet cross-section of the device is 0.04 m). The second part is a bushing with two metal grids, which reduces the level of turbulence down to 0.1%. The third part is a diffuser, which expands the flow to the diameter $D = 0.12$ m. It has two thin metal grids at the outlet to prevent the flow separation. The setup is described in detail by Zayko et al. [6].

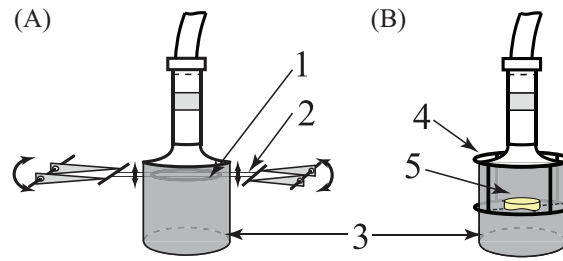


FIGURE 2 Sketches of two experimental facilities. For introduction of temporal perturbations (A): ring (1) on the strings (2) in the jet (3). The strings are oscillated by the driver in the axial direction. For introduction of stationary perturbations (B): the diffuser holder (4), deflector (5) in the jet (3). The deflector and the ring are located coaxially with the jet.

There is an optimal range of Reynolds numbers for the considered flow, in which the length of the laminar region is maximal ($\geq 5D$) so that it is possible to track the evolution of introduced perturbations at long distances from the orifice. In this study, one regime from this range is selected, in which the air flow has velocity at the jet axis $U_c = 1.5$ m/s and average velocity $U_{avg} = 0.66$ m/s, which corresponds to the Reynolds number based on the average velocity and diameter $Re_D = 5400$, and to the Reynolds number based on the maximum velocity and jet radius $Re = 6122$. The experimental velocity profile at the orifice is approximated by a cubic spline for theoretical study (Figure 1C). The downstream evolution of the unperturbed jet profile is weak and is not taken into account in the theoretical analysis [7].

2.2 | Introduction of temporal perturbations

Axisymmetric perturbations are the fastest growing perturbations of the considered jet and the most convenient to introduce them into the flow. We introduce the perturbations mechanically: two thin metal strings were pulled on two drivers at a distance $z = 19$ mm ($\approx 0.16D$, $D = 0.12$ m) from the diffuser orifice, and a ring made of a wire was fixed on the strings coaxially with the jet (Figure 2A).

The oscillations are governed by the drivers, and they have specified amplitudes and frequencies. In each series of experiments, one of the two rings was used. The first ring had a diameter of 102.4 mm ($0.85D$), and the second ring had a diameter of 56.9 mm ($0.47D$). We chose these specific diameters to locate the first (large) ring between the two outer generalized inflection points, which merge together at the small distance from the orifice producing the first branch of growing perturbations, and the second (small) ring approximately under the internal generalized inflection point, which produce the second branch. Thus, the large and small rings have to amplify the disturbances of the first and second branches, respectively.

2.3 | Introduction of stationary perturbations

To initiate the non-modal mechanism of perturbations growth, the cross-section distribution of axial velocity perturbation component could qualitatively replicate the same distribution for calculated optimal perturbations (see fig. 7 at Ivanov et al. [20]) containing the zones of particles speeding-up and slowing-down so the longitudinal vortex pairs to create. It is also known that stationary perturbations have larger non-modal growth than non-stationary ones [17]. That is why disturbances were introduced into the jet using motionless thin wave-like structures, which we will call deflectors.

The upper edge of the deflectors was a circle of radius $r_0 = D/4$ ($= 30$ mm), and the lower edge is a perturbed circle with a given azimuthal wave number n and radius $r = r_0(1 + \varepsilon \sin(n\theta))$, where ε defined the dimensionless amplitude of deviation from the circle and θ was a polar angle. The height of the deflector between the upper and lower edges is $h = D/12$ ($=10$ mm) while the wall thickness was $0.005D$ ($=0.6$ mm). A smooth transition was made between the edges (points of the upper and lower edges with the same azimuthal coordinate θ were connected by straight line segments). The models were designed in a CAD program and then 3D printed from PLA plastic.

A special holder was designed for their installation inside the jet (Figure 2B-4). The lower edge of the deflectors lay on strained fishing lines of 0.05-mm diameter. The deflectors were installed inside the jet coaxially, with the inlet edge at a distance of $z \approx 0.17D$ ($=20$ mm).

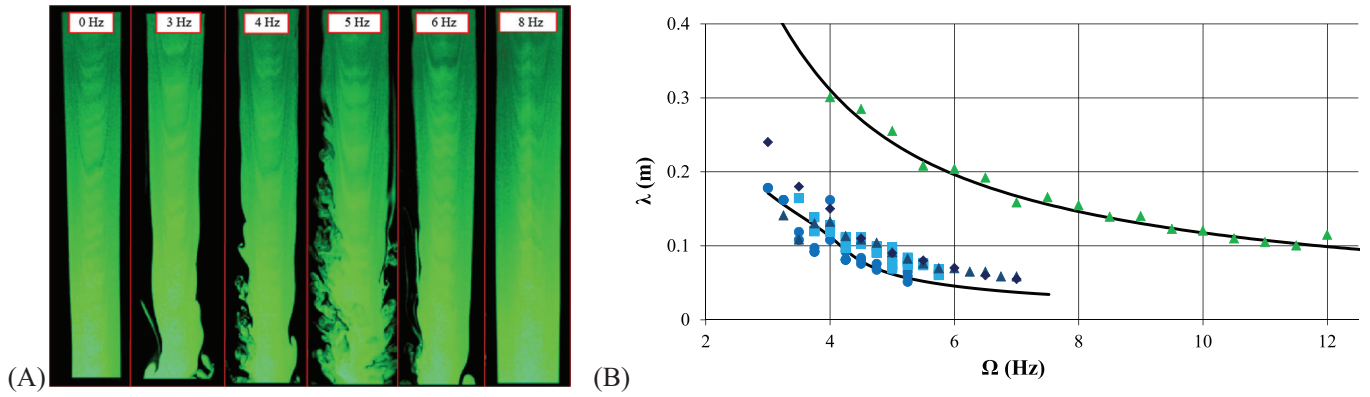


FIGURE 3 Photographs of the jet under the oscillations of the first (large) ring with different frequencies at a constant amplitude of the velocity of the ring's oscillations (A). Comparison of the theoretical (curves) and experimental (markers) wavelengths of the first branch's and second branch's disturbances (B).

3 | EXPERIMENTAL RESULTS

3.1 | Investigation of the modal mechanism

3.1.1 | Length of the laminar region

As the direct visualization shows (Figure 3A), the oscillations of the first ring significantly shorten the laminar region of the jet for frequencies $\Omega \approx 5$ Hz that correspond to the theoretical frequency range of the fastest growing perturbations of the first branch (see fig. 7 at Gareev et al. [7]).

In contrast, for frequencies lower than 4 Hz and greater than 6 Hz, the effect of the ring oscillations decays with decreasing and increasing frequency, respectively (for more detailed sequence of screenshots, see fig. 14 at Gareev et al. [7]). We see little impact on the jet: there are sinusoidal waves on the jet boundary, but they do not develop into Kelvin–Helmholtz billows and do not destroy the flow before the axial position at which the velocity fluctuations increase without the excitation; namely, before $x/D = 5$ [6]. Note that the unperturbed jet looks laminar even at a distance of $6D$ from the orifice, but the velocity fluctuations are no longer small in this area. For the other frequencies shown in Figure 3A, there is no effect of the excitation at all.

3.1.2 | Perturbations wavelengths

Wavelengths of the first-mode perturbations, which were obtained from the correlation maps and from the visualization, are in good agreement with each other and with the theoretically predicted wavelengths through the linear-stability analysis, as seen in Figure 3. This figure shows theoretical curves for the velocity profiles at distances $x/D = 0.5$ for the both branches. For the second branch, experimental values were obtained only by correlation map technique. At the same amplitude as for the large ring, there was no visually noticeable perturbation of the jet boundary; that is, the second mode was localized inside the jet. Nevertheless, there is an excellent agreement between the experimental points and the theoretical results.

3.1.3 | Radial distribution of velocity fluctuations

For the first branch, the experimental radial distributions of the velocity fluctuations (band-pass filtered near the value of the ring oscillation frequency) at distances $x/D = 0.5$ and 1 correspond to the theoretical radial distributions of the amplitude F of the axial velocity fluctuation $u_x(x, r, t) = F(r)e^{i(\alpha x - \omega t)}$, obtained in calculations with the profiles at the same distances (Figure 4). The difference between the theoretical and the experimental results near the jet boundary

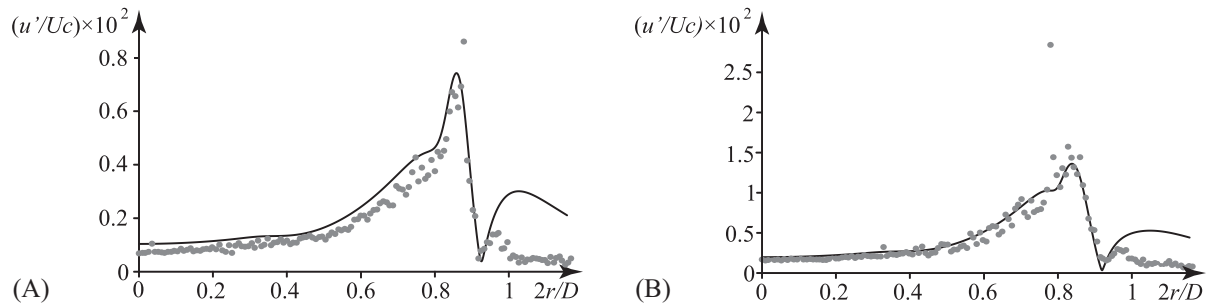


FIGURE 4 Radial distributions of the theoretical axial amplitude $|F|$ of the first branch's growing waves (curves) and of the velocity fluctuations u'/U_c obtained in the experiments with the large ring (points). Calculations with mean profiles and similar measurements for $x/D = 0.5$ (A) and 1 (B). Results with $\Omega = 4$ Hz are shown here as example.

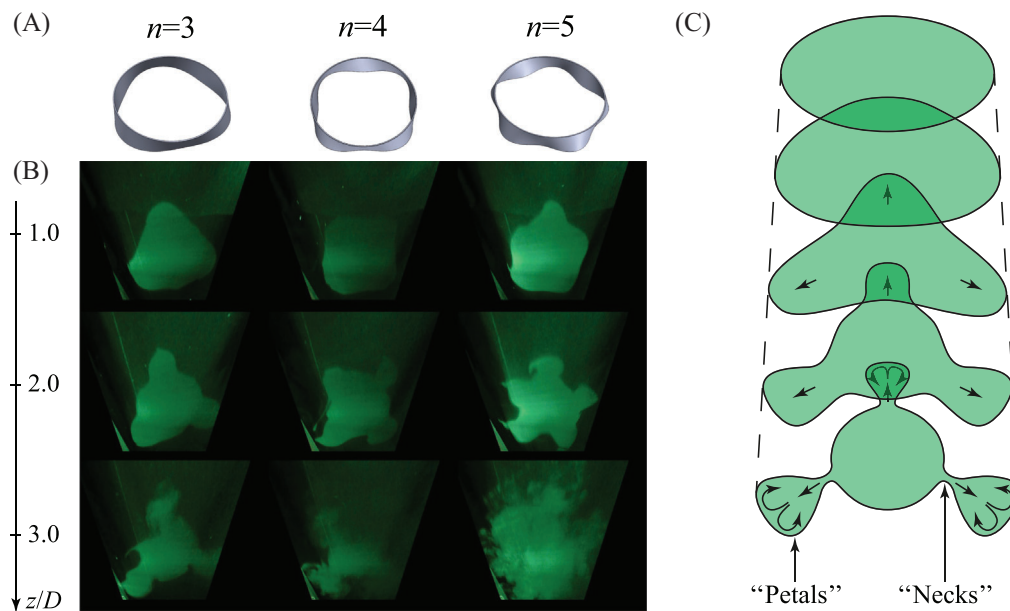


FIGURE 5 3D models of deflectors with azimuthal numbers $n = 3, 4, 5$ (A) and the evolution of stationary perturbations introduced by them at cross-section photographs (B) and at the qualitative scheme (C).

($2r/D \approx 1$) is caused by the difference between the actual velocity distribution and the unidirectional profiles used in the calculations.

Indeed, as the axial velocity becomes small near the jet boundary, it becomes comparable to the radial component caused by the viscous spreading of the jet. In other words, the flow near and outside the jet boundary is two-dimensional, which is not taken into account by the theory employed. Another source of the difference is the low accuracy of thermoanemometer measurements of small velocity values. Nevertheless, inside the jet, where the flow is truly unidirectional, the correlation between the theory and the experiments is excellent.

3.2 | Investigation of the non-modal mechanism

3.2.1 | Cross section visualization and analysis

To study the development of perturbations introduced by deflectors with $\varepsilon = 0.1$ and $d_0 = 60$ mm ($d_0 = D/2$) (Figure 5A), experiments were conducted with the visualization of the cross-sections of the jet by a laser sheet.

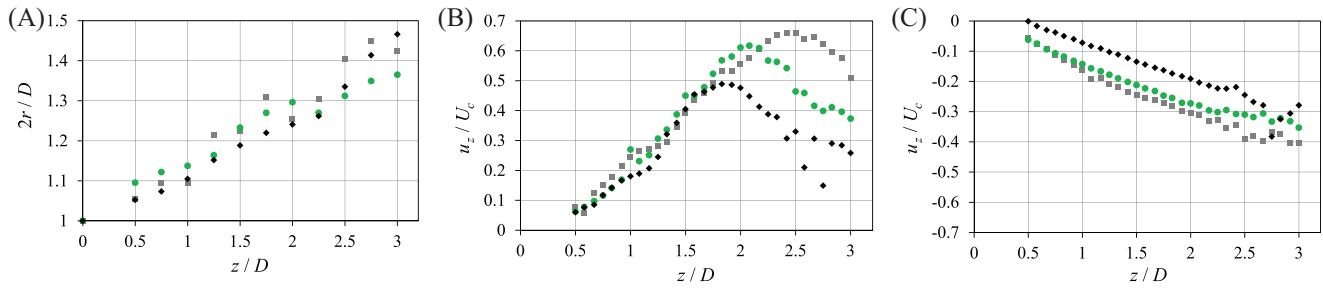


FIGURE 6 The ‘petal’ length as a function of z/D (A). Normalized axial flow velocity of perturbation versus the distance z downstream. Perturbations are introduced by a deflector with $\varepsilon = 0.1$. Measurements in ‘petals’ at $2r/D = 0.8$ (B) and ‘troughs’ at $2r/D = 0.55$ (C). Perturbations with $n = 3$ (■), $n = 4$ (○), $n = 5$ (◆).

Disturbances caused by deflectors at small distances almost do not deform the cross-section, but the cross-section changes with the development of the stationary disturbance downstream, acquiring the shape of the outlet edge of the deflectors (Figure 5B). ‘Petals’ increase, stretch in the radial direction from the jet axis and form a ‘neck’ – a narrow region of the jet section connecting the “petal” with the jet core. Shortly after the formation of “necks”, a rapid growth of unsteady fluctuations and transition to turbulence at distances $z/D \sim 3$ is observed. A qualitative scheme for the development of such perturbations is shown in Figure 5C.

PIV measurements in the transverse cut plane of the jet, which are described in Ivanov et al. [20] in detail and are not included in this short paper, showed that the evolution of introduced perturbation matches qualitative features of theoretical optimal perturbations quite well. Namely, the following characteristic features of the “lift-up” growth mechanism have been confirmed. The transverse motion has a ‘roller-like’ movement, transferring the outer layers of the fluid inward and the inner layers outward. This motion causes a local increase in the axial velocity perturbation, which is an analogue of the streaky structure in near-wall flows.

‘Petal’ lengths versus the distance z were obtained from the cross-section pictures of the jet for deflectors with $n = 3, 4, 5$, and the resulting plots are shown in Figure 6A. The lengthening of the petals occurs linearly, therefore, the radial velocity perturbation is approximately constant, which is consistent with the theoretical calculations of stationary optimal perturbations of the jet (see fig. 6a at Ivanov et al. [20]).

3.2.2 | Axial velocity downstream evolution

To make sure that the development of perturbations introduced by the deflectors qualitatively corresponds to the development of optimal perturbations, we considered the change in the axial flow velocity downstream. A series of experiments was performed to determine the average velocity with a hot-wire probe outside the flow core with deflectors for $n = 3, 4, 5$ and $\varepsilon = 0.1$ (Figure 6B,C). Points with constant radial and azimuthal coordinates were selected outside of the deflector wake.

In Figure 6B,C, the relative amplitudes of stationary disturbances versus z/D are given at the points corresponding to ‘petals’ of the jet section (left plots), and corresponding to ‘troughs’ (right plots). It is seen that in regions of contraction and expansion of the cross-section, the axial velocity evolves close-to-linearly with streamwise distance. The significant deviation from the linear growth appears only for deflectors with $\varepsilon = 0.1$ in ‘petals’ of the jet at $z/D > 2.0$. The velocity, reaching its peak at $z/D \approx 2.0$, decreases, which is explained by the growth of nonlinear effects that arise when a sufficiently large perturbation amplitude is reached; namely, by the formation of ‘necks’. Close-to-linear growth of the axial velocity is in accordance with the development of theoretical optimal perturbations (see fig. 8 at Ivanov et al. [20]).

4 | CONCLUSION

In this work, we for the first time experimentally investigated the perturbation linear growth in the long truly laminar air jet flow ($Re = 5400$) under controlled perturbations introduction. Two different perturbation growth mechanisms were considered.

1. We experimentally studied the modal mechanism of perturbations linear growth. The jet has two axisymmetric modes of instability, which were studied separately using two different oscillating rings to introduce temporal perturbations and different measuring techniques. The results are compared with eigenmode calculations of the Rayleigh equation with the parallel-flow assumption. They are in excellent agreement with theoretical analysis:
 - (a) Wavelengths of both modes;
 - (b) Radial distributions of velocity perturbations of the first mode.
2. We experimentally studied the non-modal mechanism of perturbations linear growth. The development of stationary disturbances in the jet was excited by introduction of deflectors. They caused roller-like cross-sectional stationary motion, which was qualitatively similar to optimal perturbations of the flow profile. For the first time, we experimentally identified a non-modal mechanism of the disturbances growth in a jet flow, which is an analogue of the 'lift-up' mechanism in near-wall flows. The following characteristic features of the 'lift-up' growth mechanism have been confirmed:
 - (a) Radial velocity is almost constant;
 - (b) Axial velocity downstream change is close to linear;
 - (c) The transverse motion has the form of a 'roller-like' movement – causes a local increase in the axial velocity perturbation, which is an analogue of the streaky structure in near-wall flows.

ACKNOWLEDGMENTS

This work is supported by the Russian Science Foundation under Grant 20-19-00404.

ORCID

Linar Gareev  <https://orcid.org/0000-0002-9152-5894>

REFERENCES

1. Morris, P. J. (1976). The spatial viscous instability of axisymmetric jets. *Journal of Fluid Mechanics*, 77, 511–526.
2. Shtern, V., & Hussain, F. (2003). Effect of deceleration on jet instability. *Journal of Fluid Mechanics*, 480, 283–309.
3. Mullyadzhyanov, R. I., & Yavorsky, N. I. (2018). The far field of a submerged laminar jet: Linear hydrodynamic stability. *St. Petersburg State Polytechnical University Journal. Physics and Mathematics*, 11, 84–94.
4. Cohen, J., & Wygnanski, I. (1987). The evolution of instabilities in the axisymmetric jet. Part 1. The linear growth of disturbances near the nozzle. *Journal of Fluid Mechanics*, 176, 191–219.
5. Petersen, R. A., & Samet, M. M. (1988). On the preferred mode of jet instability. *Journal of Fluid Mechanics*, 194, 153–173.
6. Zayko, J., Teplovodskii, S., Chicherina, A., Vedeneev, V., & Reshmin, A. (2018). Formation of free round jets with long laminar regions at large Reynolds numbers. *Physics of Fluids*, 30, 043603.
7. Gareev, L., Zayko, J., Chicherina, A., Trifonov, V., Reshmin, A., & Vedeneev, V. (2022). Experimental validation of inviscid linear stability theory applied to an axisymmetric jet. *Journal of Fluid Mechanics*, 934, A3.
8. Farrell, B., & Ioannou, P. (1993). Stochastic forcing of the linearized Navier-Stokes equations. *Physics of Fluids A: Fluid Dynamics*, 5, 2600–2609.
9. Andersson, P., Berggren, M., & Henningson, D. (1999). Optimal disturbances and bypass transition in boundary layers. *Physics of Fluids*, 11, 134–150.
10. Tumin, A., & Reshotko, E. (2001). Spatial theory of optimal disturbances in boundary layers. *Physics of Fluids*, 13, 2097–2104.
11. Luchini, P. (2000). Reynolds-number-independent instability of the boundary layer over a flat surface: Optimal perturbations. *Journal of Fluid Mechanics*, 404, 289–309.
12. Morkovin, M. (1984). Bypass transition to turbulence and research Desiderata. In *Nasa Conference Publication*, vol. 2386 (pp. 161–204).
13. Kendall, J. (1985). Experimental study of disturbances produced in a pre-transitional laminar boundary layer by weak free stream turbulence. In *18th Fluid Dynamics and Plasmadynamics and Lasers Conference*, AIAA.
14. Kosorygin, V., Polyakov, N., Suprun, T., & Epic, E. (1985). Influence of turbulence on the structure of perturbations in a laminar boundary layer. In *Pristenochnyye turbulentnyye techeniya* (pp. 79–83). Institute of Physics of the Siberian Branch of the USSR Academy of Sciences (in Russian).
15. Matsubara, M., & Alfredsson, P. (2001). Disturbance growth in boundary layers subjected to free-stream turbulence. *Journal of Fluid Mechanics*, 430, 149–168.
16. Boiko, A., Grek, G., Dovgal, A., & Kozlov, V. (2002). *The origin of turbulence in near-wall flows*. Springer.
17. Boronin, S., Healey, J., & Sazhin, S. (2013). Non-modal stability of round viscous jets. *Journal of Fluid Mechanics*, 716, 96–119.
18. Jiménez-González, J., Brancher, P., & Martínez-Bazán, C. (2015). Modal and non-modal evolution of perturbations for parallel round jets. *Physics of Fluids*, 27, 044105.

19. Wang, C., Lesshafft, L., Cavalieri, A. V., & Jordan, P. (2021). The effect of streaks on the instability of jets. *Journal of Fluid Mechanics*, 910, A14.
20. Ivanov, O., Ashurov, A., Gareev, L., & Vedeneev, V. (2023). Non-modal perturbation growth in a laminar jet: an experimental study. *Journal of Fluid Mechanics*, 963, A8.

How to cite this article: Gareev, L., Vedeneev, V., Ivanov, O., Zayko, J., Ashurov, D., Reshmin, A., & Trifonov, V. (2023). Experimental study of perturbation growth in a round laminar jet. *Proceedings in Applied Mathematics and Mechanics*, 23, e202300283. <https://doi.org/10.1002/pamm.202300283>